BIORESEARCH OPEN ACCESS
Volume 1, Number 1, 2012

DOI: 10.1089/biores.2012.0209

Differentiation of Human Neural Progenitor Cells in Functionalized Hydrogel Matrices

Andrea Liedmann, Stefanie Frech,* Peter J. Morgan,# Arndt Rolfs, and Moritz J. Frech

Abstract

Hydrogel-based three-dimensional (3D) scaffolds are widely used in the field of regenerative medicine, translational medicine, and tissue engineering. Recently, we reported the effect of scaffold formation on the differentiation and survival of human neural progenitor cells (hNPCs) using PuraMatrix™ (RADA-16) scaffolds. Here, we were interested in the impact of PuraMatrix modified by the addition of short peptide sequences, based on a bone marrow homing factor and laminin. The culture and differentiation of the hNPCs in the modified matrices resulted in an approximately fivefold increase in neuronal cells. The examination of apoptotic and necrotic cells, as well as the level of the anti-apoptotic protein Bcl-2, indicates benefits for cells hosted in the modified formulations. In addition, we found a trend to lower proportions of apoptotic or necrotic neuronal cells in the modified matrices. Interestingly, the neural progenitor cell pool was increased in all the tested matrices in comparison to the standard 2D culture system, while no difference was found between the modified matrices. We conclude that a combination of elevated neuronal differentiation and a protective effect of the modified matrices underlies the increased proportion of neuronal cells.

Key words: neuronal differentiation; PuraMatrix; ReNVM cells; tissue engineering

Introduction

Hydrogel-based scaffolds are widely used in the field of stem cell research, providing *in vitro* model systems that study different aspects as tissue regeneration,[1,2] self-renewal, and differentiation of stem cells.[3–6] Hydrogels consisting of synthetic nanofibres are excellent tools that generate such model systems, as they contain defined components, such as amino acids, resulting in a high reproducibility, and more over, they can be fabricated free of any animal products. Such scaffolds comprise three-dimensional (3D) networks of overlapping nanofibres, and have proved to be an effective environment for neural cells.[7–11] Their mechanical properties, for example stiffness and flexibility, can be adjusted to the needs of the hosted cells. Pore sizes ranging between 50 and 100 nm allow the diffusion of gases, metabolites, and macromolecules for nutrition. In addition, 3D scaffolds of a consistent composition with predictable properties are ideal for combination with biometric cues. Such functionalized scaffolds have been used to study critical cell functions such as proliferation, differentiation, and migration of cells within the 3D-culture systems.[12–14] A well-described hydrogel-based self-assembling scaffold, complying with the properties just mentioned, is PuraMatrix™ (RADA16-I). PuraMatrix (PM) was used in a series of studies to investigate proliferation and neuronal differentiation with stem and progenitor cells of different origins.[15–18]

The next generation of self-assembling scaffolds is featured by the functionalization of the self-assembling backbone sequences with specific biological motifs.[19–21] Laminin-derived sequences have been shown to be supportive of neuronal differentiation and survival when inserted into scaffolds.[22] Functionalization of PuraMatrix with different short peptides, including among others a laminin-derived sequence (-GGSDPGYIGSR-) and a sequence found in the bone marrow homing factor (-GGPFSSTKT-), was shown to affect the mechanical properties of the matrix and alter neuronal differentiation.[15,16,23] In a recent study, we supplemented PuraMatrix with laminin and described the fate of human neural progenitor cells (hNPCs) encapsulated in these 3D scaffolds, regarding differentiation and survival.[24,25] Based on those findings, here we have tested the influence of modified

Albrecht-Kossel-Institute for Neuroregeneration, University of Rostock, Rostock, Germany.
*Current address: Bionas GmbH, Rostock, Germany.
#Current address: Erasmus MC, Department of Neuroscience, Rotterdam, The Netherlands.

formulations of PuraMatrix (kindly provided by BD) on the neuronal differentiation of human NPCs. We used the immortalized hNPC line ReNcell VM (Millipore). This cell line has been described as an *in vitro* model system in a variety of studies dealing with neuronal differentiation in standard culture systems,[26–32] as well as in 3D scaffolds,[24,25] though the immortalization precludes any application in human studies. The cell line is characterized by a fast proliferation and a rapid onset of differentiation on the withdrawal of growth factors.[32] The hydrogel was modified by the addition of short peptide sequences to the backbone, modifications that have been shown to influence the adhesion and differentiation of mouse neural stem cells *in vitro*.[16,23] In this study, we were interested in the influence of the modifications on the differentiation of the hNPCs. Therefore, we proliferated and differentiated the cells in standard and two modified formulations of PuraMatrix. To overcome obstacles regarding the analysis of the cells hosted in the matrices, we adapted a protocol that releases the cells from the 3D scaffolds[25,33] and subsequently analyzed the amount of neuronal cells and different parameters, for example, the amount of apoptotic cells by means of flow cytometry.

Methods

Culture of hNPCs in 3D scaffolds

The hNPCs were cultured as previously described.[32] In short, the cells were cultivated in Dulbecco's modified eagle medium /F12), supplemented with Glutamax, B27 media supplement, heparin sodium salt, and gentamycin (all Invitrogen). During proliferation, epidermal fibroblast growth factor (eFGF, 20 ng/mL) and basic fibroblast growth factor (bFGF, 10 ng/mL, both Roche) were added to the media. hNPCs were proliferated for 4 days and, subsequently, embedded in the 3D scaffolds as previously described.[24,25] The hNPCs were proliferated for 7 days in all scaffolds. Differentiation was induced by the withdrawal of growth factors. The cells were differentiated for approximately 10 days with the media changed every 2–3 days. Based on the results of a previous study,[24] we used a PuraMarix concentration of 0.25% to host the cells. In this study, PuraMarix and formulations (kindly provided by BD Bioscience) modified with two different peptide sequences, namely (1) -GGSDPGYIGSR- (denoted as PM-SDP) and (2) -GGPFSSTKT- (denoted as PM-PFS) were used. Nonmodified PuraMatrix is denoted as PM.

Immunocytochemistry

For immuncytochemistry, 3D cultures were fixed with paraformaldehyde (4% in 0.1 M phosphate buffered saline [PBS]) for 30 min and stored at 4°C in PBS with 0.02% NaN_3. For staining, the matrices were stored for 24 h in blocking buffer (normal goat serum 5% [NGS] + Triton X-100 0.3% in PBS) and subsequently incubated overnight with the primary antibody dissolved in PBS with 1% NGS at 4°C (βIII-tubulin, Santa Cruz, 1:500 mouse monoclonal or tyrosine hydroxylase [TH], Chemicon, 1:500, rabbit polyclonal). After washing the cells four times within 24 h, the secondary antibody, dissolved in PBS with 1% NGS, was added (Alexa Fluor 488, Molecular Probes, 1:1000, goat anti-mouse or Alexa Fluor 568, Molecular Probes, 1:1000, goat anti-rabbit), and matrices were stored for 4 h at room temperature (RT) in the dark. The samples were washed 4–6 times for 1 h followed by an overnight incubation with PBS. Cell-nuclei labeling was performed with 4',6-diamidin-2'-phenylindoldihydrochloride (DAPI, 100 ng/mL in PBS, Molecular Probes).

Subsequently, matrices were mounted with Mowiol/Dabco. For analyzing the immunofluorescence labeling, a stack of 30 single pictures was taken with a Biozero microscope (Keyence). With the corresponding analyzer software, a full projection was generated.

Flow cytometry

For flow cytometry, 3D scaffolds were mechanically disrupted, and cells were released by adding trypsin.[31] After centrifugation at 3000 *g* at RT for 5 min, the cells were washed twice with HBSS buffer. Subsequently, large cell/matrix aggregates were removed with a cell strainer (70 μm). After fixing the cells with 1% PFA for 15 min, the cells were resuspended in buffer (PBS + 0.5% bovine serum albumin [BSA] + 0.02% Na-azide). For the staining (2 h at RT), the cells were centrifuged and resuspended in saponin buffer (PBS + 0.5% saponin + 0.5% BSA + 0.02% Na-azide) containing the first antibody against the βIII-tubulin antibody (Santa Cruz, 1:100, mouse monoclonal), HuC/D (Invitrogen, 1:100, mouse monoclonal), PSA-NCAM (Millipore, 1:100, mouse monoclonal, IgM), Bcl-2 (Santa Cruz, 1:500, mouse monoclonal), or without the primary antibody providing a negative control. Afterward, the cells were washed twice with saponin buffer and incubated with the secondary antibody Alexa Fluor 647 (Molecular Probes, 1:1000, goat anti-mouse) or Alexa Fluor 488 (Molecular Probes, 1:1000, goat anti-mouse) for 1h in saponin buffer. The cells were washed again twice with saponin buffer and resuspended in wash buffer for analysis. A total amount of 50.000 cells of each probe was measured. Measurements were done using an FACSCalibur instrument (Becton-Dickinson) in combination with Cell Quest Pro software.

TUNEL assay

For TUNEL assay, we used an In Situ Cell Death Detection Kit (Roche). The cells were prepared as just described. Fixed cells (1% PFA for 15 min) were resuspended in HBSS with 0.2% HSA. Next, the cells were permeabilized (0.1% Triton X-100 + 0.1% sodium citrate in PBS) for 2 min on ice and afterward incubated in a TUNEL reaction mix for 1h at 37°C in a humidified atmosphere, in the dark. Samples were subsequently washed and stored in PBS until analysis. For positive controls, cells were incubated with DNase I (3000 IE/mL) to induce DNA strand breaks. Measurements were done using FACSCalibur (BectonDickinson) in combination with Cell Quest Pro software.

AnnexinV/propidium iodide apoptosis detection

To determine the amount of apoptotic and necrotic cells, an FITC Annexin V Apoptosis Detection Kit I (BD Bioscience) was used. Cells were released from the scaffolds as just described and washed twice with HBSS. The cells were resuspended in binding buffer (0.1 M HEPES/NaOH [pH 7.4], 1.4 M NaCl, 25 mM $CaCl_2$), and Annexin V and propidium iodide (PI) were added according to the manufacturer's manual. After 15 min incubation at RT on a shaker in the dark, the measurement was done by using FACSCalibur (Becton-Dickinson) in combination with Cell Quest Pro software.

Statistics

All statistical analysis were performed with Prism 5 (GraphPad Prism, Inc.) using one-way analysis of variance with the Bonferroni Post test. p-value ≤ 0.05 was considered as indicating significant statistical differences. Values represent mean ± s.e.m.

Results

The aim of this study was to evaluate the effects of the two modified formulations of PuraMatrix on the hNPCs. Therefore, the proportion of neuronal cells and several parameters regarding neuronal differentiation and survival of the cells were analyzed by means of flow cytometry.

Expression of neuronal markers of hNPCs in modified PuraMatrix

Since the modifications are described as influencing the differentiation of adult mouse stem cells,[23] we were interested in the effect of the modifications on the differentiation of human NPCs. Therefore, we cultured and differentiated hNPCs in PM, PM-SDP, and PM-PFS. In all three conditions, the cells grew in spheroid-like structures wherein slight differences in the growth pattern were observed by transmission light micrographs (Fig. 1A, C, E). The cells cultured in PM-PFS showed processes tending to leave the spheroid-like structures (Fig. 1C). To a certain extent, this could be observed in PM-SDP (Fig. 1E) but was hardly seen in PM (Fig. 1A).

On the induction of differentiation by the withdrawal of bFGF and eFGF, the cells started expressing the neuronal marker βIII-tub. It was striking that in both modified matrices, a higher amount of positive staining was observed in comparison to the normal PM (Fig. 1B, D, F), indicating a beneficial effect of the modified matrices on the differentiation of the hNPCs. The cells differentiated in PFS displayed the highest amount of βIII-tub$^+$ cells and developed a very dense network of processes (Fig. 1D). Based on these results, the amount of neuronal cells in the scaffolds consisting of PM, PM-SDP, or PM-PFS was investigated.

Amount of neuronal cells in scaffolds consisting of different PM formulations

Recently, we demonstrated that the formation and structure of 3D scaffolds can impact the neuronal differentiation, where we performed immunocytochemical staining and determined the percentage of neuronal cells by manual counting.[24] Since this method is extremely time consuming and only a small proportion of the cells can be analyzed, we adapted a method that extracts cells from 3D scaffolds and subsequently examines them by means of flow cytometry.[25] We quantified the cells cultured in scaffolds consisting of PM, PM-SDP, and PM-PFS. An unstained sample (Fig. 1G) was used to determine the proper gate for the analysis of positive cells (Fig. 1H).

As evident from the fluorescence pictures (Fig. 1B, D, F), the quantification of βIII-tub$^+$ cells revealed significantly higher proportions of positive cells in the PM-SDP and PM-PFS scaffolds in comparison to the PM scaffolds (Fig. 2A). After 4 days of differentiation (dd), we detected 17.7% ± 3.3% of βIII-tub$^+$ cells in PM-SDP and 21.9% ± 4.2% in PM-PFS in comparison to 3.7% ± 0.9% of βIII-tub$^+$ cells in PM. The difference was significant between PM and the modified formulations but not between the PM-SDP and PM-PFS; however, a slightly higher number was observed in PM-PFS. Interestingly, the amount of βIII-tub$^+$ cells was stable over time in the modified matrices, where the number of cells in the PM scaffolds was increasing until the latest analyzed time point of 10 days. At this stage, the amount of βIII-tub$^+$ cells was twice to thrice higher in PM-SDP and PM-PFS compared with PM. Noticeably, we observed βIII-tub$^+$ cells in proliferating cells (day 0) in PM-SDP (2.8% ± 0.6%) and PM-PFS (3.3% ± 0.6%), most likely indicating the spontaneous differentiation of the cells in the modified matrices.

To consolidate these findings, we used an antibody against the human neuronal protein (HuC/D) as another marker for neuronal cells (Fig. 2B). We found a higher amount of positive cells at certain time points. After 4 dd, we found 7.4% ± 2.2% positive cells in PM, 9.9% ± 2.5% in PM-SDP, and 11.7% ± 1.6% positive cells in PM-PFS, where the amount was not significantly different. We found a significantly higher proportion of positive cells in PM-PFS after 7 dd in comparison to PM. In contrast to the results of the βIII-tub staining, the number of HuC/D$^+$ cells was declining in PM scaffolds after 4 dd, where the number of positive cells in PM-SDP and PM-PFS changed at certain time points; however, the number of neuronal cells was always lower in PM in comparison to the modified scaffolds. Since HuC/D is described as marking cells shortly after their leaving the cell cycle, these results might indicate different developmental states in the different scaffolds. As a next step, we wanted to elucidate the mechanism contributing to the higher proportion of neuronal cells in PM-SDP and PM-PFS matrices.

Expression of Bcl-2 in scaffolds consisting of different PM formulations

Anticipating a protective effect of the modified matrices on the cells, we analyzed the amount of the anti-apoptotic protein Bcl-2. The cells that were released from each type of scaffold were analyzed by means of flow cytometry (Fig. 3). The analysis revealed a significant increase between day 0 (proliferating cells) and the cells differentiated for 4 days in all conditions. After 4 dd, the level of Bcl-2 changed only slightly in all conditions, though there was a prominent, but not significant, decline at days 7 and 10 in PM-SDP (Fig. 3, gray bars). With this exception, the lowest amount at the different time points was always detected in the scaffolds consisting of PM-PFS.

Amount of apoptotic and necrotic cells in the different matrix formulations

To further investigate a possible protective effect of the PM formulations on the hNPCs, we next analyzed the proportion of apoptotic and necrotic cells. We used an AnnexinV and PI staining to determine the amount of cells in an early apoptotic state (AnnexinV positive), a late apoptotic state (AnnexinV/PI positive), and the amount of necrotic cells (PI positive). Comparable to the level of Bcl-2, we found an increase of AnnexinV$^+$ cells between day 0 (proliferating cells) and day 4 in all conditions (Fig. 4A). Although we had observed an increase in the different scaffolds, neither the difference between the formulations nor the difference between later time points was significant, most likely

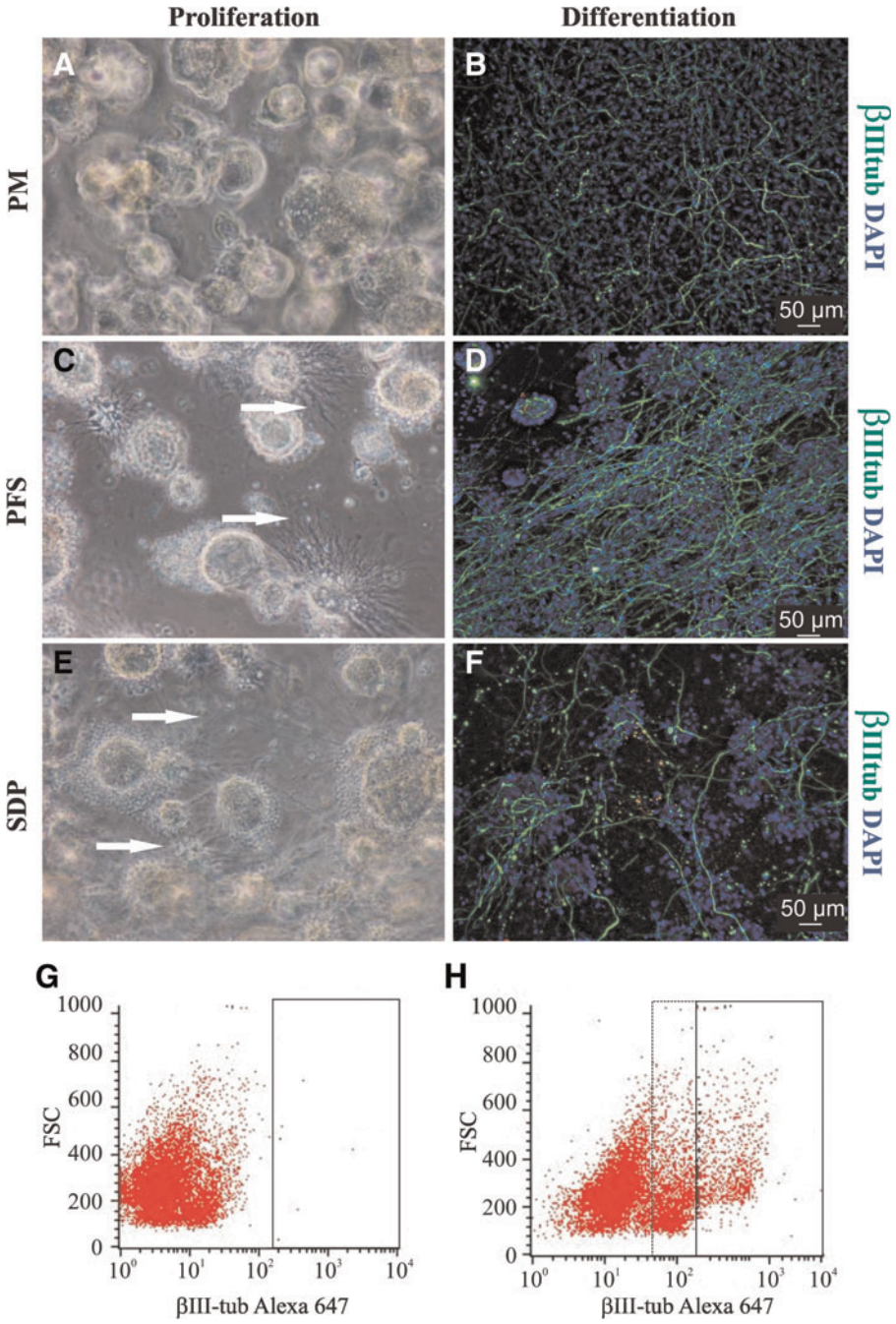

FIG. 1. Culture of hNPCs in 3D scaffolds. hNPCs proliferated for 7 days in PuraMatrix™ **(A)** and modified formulations of PuraMatrix **(C, E)**. hNPCs encapsulated in all three different formulations of PM grown in spheric, densely packed structures, where the diameter of the spheres can be approximately several 100 μm. Although one can observe comparable patterns of the matrices, the cells grown in PM-PFS or PM-SDP tend to send more processes to the outer side of the spheroids (indicated by arrows in **C** and **E**). After 7 days of differentiation, the expression of the neuronal marker betaIII-tub was observed in all three conditions **(B, D, F)**, whereas a higher density of processes and cell bodies was observed in matrices consisting of PM-PFS or PM-SDP **(D, F)**. For the flow cytometry analysis of hNPCs, the cells were released from the 3D scaffolds. **(G)** Unstained cells were used as a negative control, to set the gate (black frame) for the subsequent analysis of, for example, βIII-tubulin$^+$ cells. **(H)** The same gate, as set in the negative control, was used to quantify the amount of βIII-tubulin$^+$ cells. Positive cells appear in the right part of the x-axis, where and intermediate population also was observed (dotted frame), most likely representing the debris of cells. hNPCs, human neural progenitor cells; 3D, three-dimensional.

due to the variation of the sampled data. For the amount of cells in a later stage of apoptosis, indicated by a double-positive staining for AnnexinV and PI (Fig. 4B), we observed a slight increase in double-positive cells between day 0 and day 4, followed by a slight decrease in positive cells over time, for all scaffolds. We found no significant differences between the scaffolds or over the time. Next, we analyzed the proportion of necrotic cells indicated by PI-positive cells (Fig. 4C). In all three types of scaffolds, we found an increase in necrotic cells between day 0 and day 4. In PM-SDP and PM-PFS scaffolds, the proportion of PI-positive cells declined between day 7 and day 10, where the number of necrotic cells in PM-PFS never reached the level of the necrotic cells in PM or PM-SDP. Moreover, the level of PI-positive cells did not decline but rather increased in the scaffolds consisting of PM. This result suggests that at least a certain proportion of the increased number of neuronal cells in the modified matrix formulations is based on a protective influence of the modified scaffolds.

Proportion of TUNEL-positive neuronal cells in the different matrix formulations

Since we had obtained the amount of Bcl-2$^+$ cells and the proportion apoptotic/necrotic cells from the whole population of cells hosted in the matrices, we next analyzed the

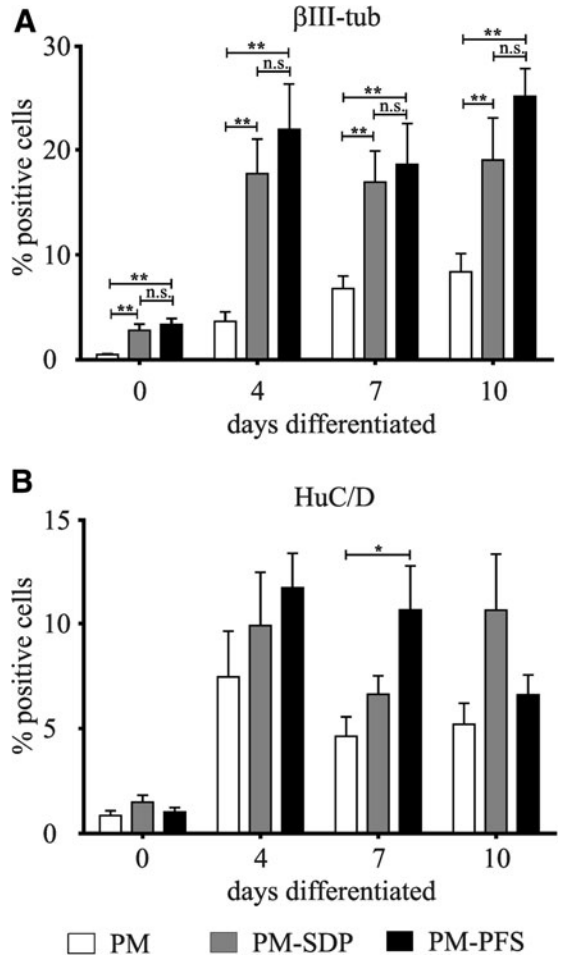

FIG. 2. Quantification of neuronal cells. Comparison of the amount of neuronal cells hosted in the different PM formulations. To determine the size of the neuronal population, we used the neuronal marker βIII-tub and HuC/D. **(A)** The flow cytometry analysis revealed a significantly higher amount of βIII-tub$^+$ cells in the modified formulations PM-SDP (gray bars) and PM-PFS (black bars) in comparison to PM (white bars). Notably, the peak of neuronal cells in PM-SDP and PM-PFS was reached after 4 dd and was stable until the latest time point of observation (10 dd), whereas the amount of βIII-tub$^+$ cells tend to increase over time in PM. **(B)** As a second neuronal marker, we used HuC/D. Comparable to the analysis of βIII-tub$^+$ cells, we found a higher number of positive cells in the PM-SDP and PM-PFS. *$p \leq 0.05$; **$p \leq 0.01$. n.s., not significant; dd, days of differentiation.

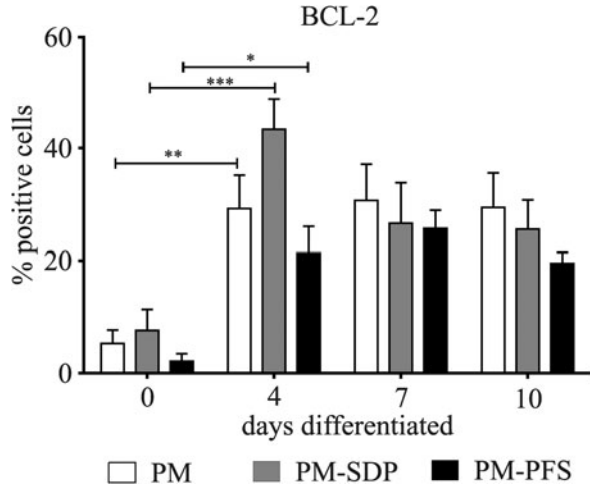

FIG. 3. Quantification of Bcl-2. Determination of the anti-apoptotic protein Bcl-2. To test the hypothesis of a protective effect on the modified PM formulations, we analyzed the amount of the anti-apoptotic protein Bcl-2 by flow cytometry. In all three conditions (PM [white bars], PM-SDP [gray bars], PM-PFS [black bars]), we observed a significant increase of the Bcl-2 level after 4 dd. After 10 dd, the lowest amount was found in scaffolds consisting of PM-PFS (19.5 ± 1.9), and the highest amount was found in PM scaffolds (29.4 ± 6.2), indicating a benefit of the PM-PFS scaffolds over PM scaffolds, with regard to a protective effect. *$p \leq 0.05$; **$p \leq 0.01$; ***$p \leq 0.001$.

amount of neuronal cells undergoing apoptosis or necrosis by means of a combination of a TUNEL assay and βIII-tub staining. The quantification was done by means of flow cytometry measurements, and the percentage of TUNEL$^+$ cells within the population of βIII-tub$^+$ cells was determined. The analysis of cells released from PM revealed an increase of TUNEL$^+$ and βIII-tub$^+$ cells from 41.1% ± 18.7% at day 0 (proliferating cells) up to 89.4% ± 5.6% after 10 dd (Fig. 5, white bars). The amount of double-positive cells at day 0 released from PM-SDP (Fig. 5, gray bars) and PM-PFS (Fig. 5, black bars) was comparable to those of PM (PM-SDP 34.1% ± 14.6% and PM-PFS 25.3% ± 9.4%). After 10 dd, the amount was lower in PM-SDP (65.9% ± 18.2%) and PM-PFS (59.8% ± 18.8%), where the amount changed only slightly over time in PM-SDP and PM-PFS but increased over time in PM. Although we observed this clear tendency, the differences were not significant. However, these data suggest a neuroprotective effect of the modified matrices PM-SDP and PM-PFS, which can contribute to the overall higher amount of neuronal cells in these scaffolds. Taken together, these results indicate that the modified matrices support the survival of the cells, although we only could describe a tendency. As a further possible mechanism contributing to the higher amount of neuronal cells, we asked ourselves whether a change in the cell pool directed toward neuronal differentiation contributes to the observed increase in neuronal cells.

Analysis of progenitor cell pool in scaffolds consisting of different PM formulations

To determine the size of the progenitor pool directed toward neuronal differentiation, we analyzed the amount of PSA-NCAM$^+$ cells (Fig. 6). The hNPCs were proliferated for 7 days in the scaffolds and thereafter released and analyzed by means of flow cytometry. The highest amount of PSA-NCAM$^+$ cells was found in the scaffolds consisting of PM, namely 49.5% ± 8.6%. PM-SDP and PMPFS-scaffolds contained 32.2% ± 5.3% and 43.0% ± 3.0% positive cells, respectively. However, the differences between the different scaffolds were not significant. In addition, we analyzed the amount of PSA-NCAM$^+$ in standard 2D cultures (5.8% ± 1.6%), which was five to eight times lower compared with the 3D scaffolds. Accordingly, we found a much lower number of neuronal cells in the 2D cultures (data not shown).

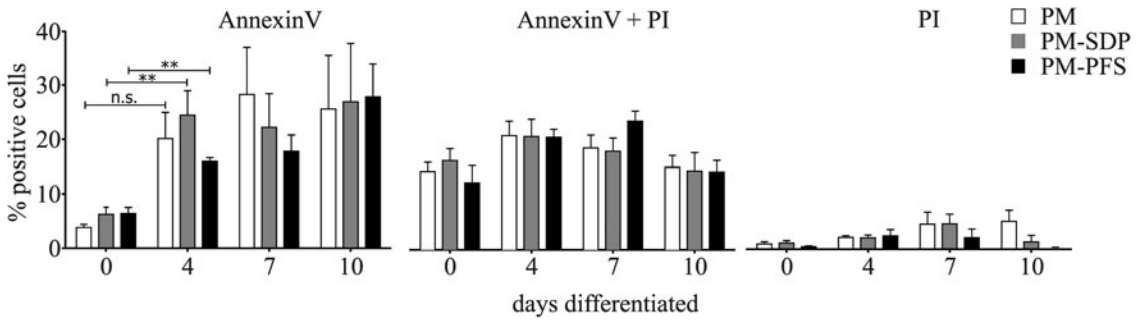

FIG. 4. Quantification of apoptotic and necrotic cells. Determination of apoptotic and necrotic cells in the different PM formulations (□, PM; ▒, PM-SDP; ■, PM-PFS). To evaluate the amount of apoptotic and necrotic cells, we used an AnnexinV/PI staining, where AnnexinV is the marker for apoptotic cells, and PI is the marker for necrotic cells. The flow cytometry analysis revealed a significant increase in the number of cells in an early state of apoptosis (AnnexinV positive) in the modified matrices. No differences were found between the different matrices for the later time points. No increase or difference between the time points was observed for cells in the late apoptotic state (AnnexinV and PI positive) or necrotic cells (PI positive) in all three formulations of PM. $^{**}p \leq 0.01$. PI, propidium iodide.

Discussion

The influence of 3D scaffolds on growth, proliferation, and neuronal differentiation is of great interest in order to find new methods for cell-based therapies. In the context of regenerative medicine, the combination of biomaterial scaffolds with neural stem and progenitor cells holds great promise as a therapeutic tool.[13,34–37] Culture systems emulating a 3D environment have been shown to influence proliferation and differentiation in different types of stem and progenitor cells. Here, the formation and functionalization of the 3D microenviroment is important for the survival and fate of the embedded cells.[15,16] PuraMatrix (RADA16), a peptide-based hydrogel scaffold, has been well described and used to study the influence of a 3D environment on different cell types.[15–18] Recently, we have demonstrated the impact of the formation of PuraMatrix on the survival and differentiation of hNPCs.[24,25] The combination of biodegradable scaffolds as PuraMatrix and hNPCs is of special interest, as scaffolds can be fabricated xeno free and in a highly standardized manner in comparison to animal-derived products with a high batch variability.[38,39]

In this study, we used two modified formulations of PuraMatrix, wherein both formulations of short peptide sequences were linked to PuraMatrix. In PM-SDP, the peptide sequence—SDPGYIGSR—was added, which is a motif found in laminin and described as promoting cell adhesion and the

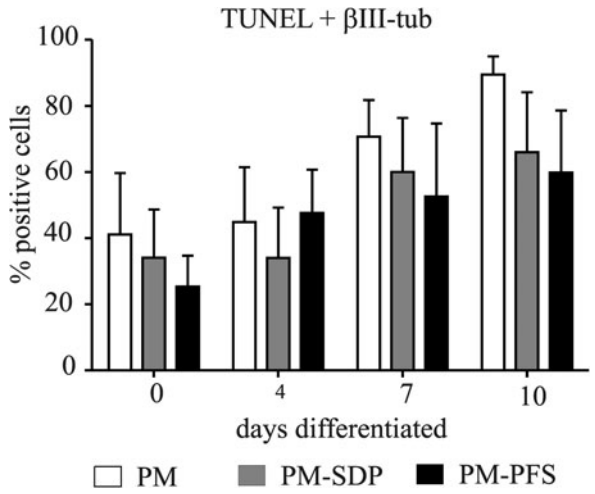

FIG. 5. Quantification of apoptotic neuronal cells. Evaluation of TUNEL$^+$ and βIII-tub$^+$ cells. Since the determination of Bcl-2 or AnnexinV/PI was based on total cell population, we analyzed the amount of cells that were double positive for TUNEL staining and βIII-tub, indicating the neuronal population. In all three scaffold formulations, we observed an increase in the double-positive cells over time. The highest number of double-positive cells was found after 10 dd in all conditions, where the highest level was observed in PM scaffolds, and the lowest level was observed in PFS scaffolds (PM 89.4% ± 5.6% vs. PM-PFS 59.8% ± 18.8%).

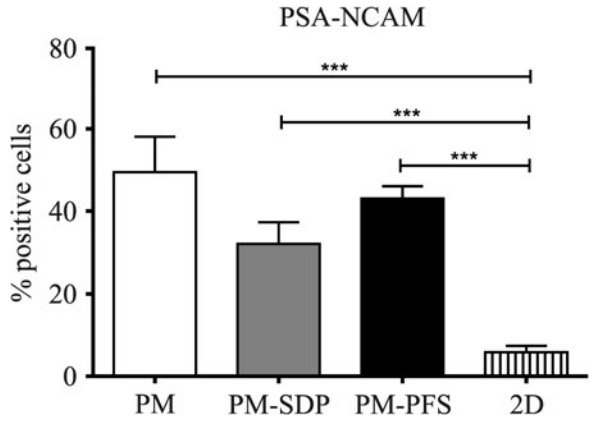

FIG. 6. Quantification of neural progenitor cell pool. Determination of the neural progenitor pool in the different PM formulations. As one possible underlying mechanism for the elevated number of neuronal cells, we hypothesized an influence of the modifications on the progenitor pool. Therefore, we determined the amount of PSA-NCAM$^+$ cells with flow cytometry. The measurement revealed no significant differences between the three formulations of PM. However, the highest amount was found in PM (□). In addition, we analyzed the amount of positive cells in standard 2D cultures and found a significantly lower amount of PSA-NCAM$^+$ cells (▥). $^{***}p \leq 0.001$.

extensibility of neural cells.[40–43] The second modification consists of the addition of the peptide sequence -GGPFSSTKT- a motif of the bone marrow homing factor that is shown to stimulate neuronal stem cell adhesion and differentiation *in vitro*.[16] Both modified matrices have been used to promote the proliferation and differentiation of adult mouse neural stem cells.[16,23] In accordance with the results of Cunha et al., we found a significantly increased amount of neuronal cells in both modified matrices, where in PM-PFS an approximately sevenfold increase was observed (Fig. 2A). The modifications are discussed to change the 3D structures of the matrices, resulting in changed mechanical properties as stiffness or flexibility. It was recently reported that the mechanical properties of a matrix can determine the fate of cells toward a neuronal phenotype (soft gels) or an osteogenic differentiation (hard gels).[44–46] The stiffness of the matrices comparable to the matrices used here showed no differences,[47] most likely ruling out a contribution to the observed increase in neuronal cells.

Besides changes in the mechanical properties of matrices due to modifications, changes in the permeability of a matrix might result in a more effective delivery of nutrients and oxygen to the cells[11] and, thus, an improvement in the survival rate of cells. Based on this assumption, we determined parameters indicating the level of apoptotic or nectrotic cells cultured in the different matrices by means of flow cytometry.

We observed the tendency of a higher survival rate of the cells in the modified matrices, although we did not find significant differences between the modified matrices and the nonmodified PuraMatrix. Consistently, we found a trend toward higher amounts of apoptotic cells and a higher proportion of apoptotic/nectrotic neuronal cells in PM in comparison to the modified matrices PM-SDP and PM-PFS.

As recently described, the used hNPCs can be protected by the Na^+-channel agonist Veratridine,[27] indicating a protective effect depending on the activity of neuronal cells in the culture system. In addition, we described a changed functionality of the cells co-cultured with hippocampal brain slices, where we found the cells that receive synaptic input from the host tissue proofing the expression of neurotransmitter receptors.[28] The importance of the expression of neurotransmitter receptors in very early developmental stages of neurons or even neuroblasts is shown to be important for the survival of the cells in an increasing number of studies.[48–52] For human mesencephalic NPCs, it was shown that a persistent application of the glutamate receptor agonist NMDA during the proliferation results in an increased number of TH immunopositive cells, indicating activity-dependent mechanisms.[52] Similar results were obtained in a study using cortical NPCs.[53] Taken together, one can deduce that NPCs need neuronal activity or a certain level of neurotransmitters to survive and mature. To support the idea that an increased neuronal activity might contribute to the higher amount of neuronal cells we observed in the modified matrices, we performed patch-clamp studies. Therefore, the cells were differentiated within the matrices, subsequently released, and plated on cover slips, as the cells situated in the scaffolds cannot be accessed for such studies. First, results indicated and evaluated the number of cells expressing functional Na^+ channels (data not shown). However, further studies are necessary to elucidate differences in synaptogenesis and, subsequently, neuronal network activity determined, for example, by recording the synaptic currents underlying neuronal network activity.

Another aspect is that a higher density of cells leads to an improvement of cell-cell interactions. Cell-cell interactions play a crucial role in the proliferation, development, and survival of cells[54,55] and might contribute to the higher amount of neuronal differentiation observed in the modified matrices.

Besides investigating the protective effects of the matrices, we asked whether the pool of neural-determined progenitor cells contributes to the higher amount of neural-differentiated cells. We used PSA-NCAM as a marker for cells that were determined to undergo neuronal differentiation. Although PSA-NCAM is not solely a marker for neuronal progenitor cells but also for glial progenitors,[56–58] it was used for neuronal lineage selection in the past.[59–63] Recently, it was shown for human ES cells that a preselection of PSA-NCAM-positive cells results in highly purificated neuronal lineages, where the size of the PSA-$NCAM^+$ pool increased over the time of differentiation, indicating an increasing pool of neuronal cells.[64] In contrast, we found in our study that the level of PSA-$NCAM^+$ cells did not change on the induction of differentiation (data not shown). Furthermore, we found no significant differences in the pool of PSA-NCAM-positive cells in proliferating cells (Fig. 6) within the different matrices. However, interestingly, we found a five to eight times higher amount of PSA-$NCAM^+$ cells in the 3D scaffolds compared with cells cultured in a 2D monolayer system (Fig. 6). This leads us to the conclusion that the 3D environment, regardless of the composition used, has a massive impact on the neuronal fate-determined progenitor pool, although the underlying mechanism remains unknown, and that the modified matrices PM-SDP and PM-PFS possess benefits over the PM regarding the survival of differentiated cells over time.

In summary, our results demonstrate the importance of a lineage-specific proliferation, as shown by the impact of a 3D culture system on the pool of neuronal fate-determined cells. Furthermore, we have shown the beneficial influence of the environment on the survival of hosted cells. Taken together, these results demonstrate that the 3D scaffolds might provide a powerful tool for optimizing the yield of neural progenitors, and subsequent neuronal differentiation, for research and therapeutic applications.

Acknowledgments

The authors thank Ellen Ewald and Norman Krüger for their excellent technical support. They also thank BD Bioscience for the kind gift of the modified PuraMatrix formulations PM-SDP and PM-PFS.

Authors' Contribution

A.L. designed the study, performed experiments, analyzed data, and wrote the article. P.J.M. designed the study, performed experiments, and analyzed data. S.F., A.R., and M.J.F. designed the study, analyzed data, and wrote the article.

Author Disclosure Statement

The authors have nothing to disclose.

References

1. Novikova LN, Mosahebi A, Wiberg M, et al. Alginate hydrogel and matrigel as potential cell carriers for neurotransplantation. J Biomed Mater Res A. 2006;77:242–252.

2. Prang P, Muller R, Eljaouhari A, et al. The promotion of oriented axonal regrowth in the injured spinal cord by alginate-based anisotropic capillary hydrogels. Biomaterials. 2006;27: 3560–3569.
3. Brannvall K, Bergman K, Wallenquist U, et al. Enhanced neuronal differentiation in a three-dimensional collagen-hyaluronan matrix. J Neurosci Res. 2007;85:2138–2146.
4. Gerecht S, Burdick JA, Ferreira LS, et al. Hyaluronic acid hydrogel for controlled self-renewal and differentiation of human embryonic stem cells. Proc Natl Acad Sci USA. 2007;104:11298–11303.
5. Uemura M, Refaat MM, Shinoyama M, et al. Matrigel supports survival and neuronal differentiation of grafted embryonic stem cell-derived neural precursor cells. J Neurosci Res. 2010;88:542–551.
6. Pan L, Ren Y, Cui F, Xu Q. Viability and differentiation of neural precursors on hyaluronic acid hydrogel scaffold. J Neurosci Res. 2009;87:3207–3220.
7. Martin BC, Minner EJ, Wiseman SL, et al. Agarose and methylcellulose hydrogel blends for nerve regeneration applications. J Neural Eng. 2008;5:221–231.
8. Holmes TC, de Lacalle S, Su X, et al. Extensive neurite outgrowth and active synapse formation on self-assembling peptide scaffolds. Proc Natl Acad Sci USA. 2000;97:6728–6733.
9. Semino CE, Kasahara J, Hayashi Y, Zhang S. Entrapment of migrating hippocampal neural cells in three-dimensional peptide nanofiber scaffold. Tissue Eng. 2004;10:643–655.
10. Xu XY, Li XT, Peng SW, et al. The behaviour of neural stem cells on polyhydroxyalkanoate nanofiber scaffolds. Biomaterials. 2010;31:3967–3975.
11. Owen SC, Shoichet MS. Design of three-dimensional biomimetic scaffolds. J Biomed Mater Res A. 2010;94:1321–1331.
12. Horii A, Wang X, Gelain F, Zhang S. Biological designer self-assembling peptide nanofiber scaffolds significantly enhance osteoblast proliferation, differentiation and 3-D migration. PLoS One. 2007;2:e190.
13. Gelain F, Horii A, Zhang S. Designer self-assembling peptide scaffolds for 3-d tissue cell cultures and regenerative medicine. Macromol Biosci. 2007;7:544–551.
14. Blow N. Cell Culture: Building a better matrix. Nature Methods. 2009;6:619–622.
15. Taraballi F, Natalello A, Campione M, et al. Glycine-spacers influence functional motifs exposure and self-assembling propensity of functionalized substrates tailored for neural stem cell cultures. Front Neuroeng. 2010;3:1.
16. Gelain F, Bottai D, Vescovi A, Zhang S. Designer self-assembling peptide nanofiber scaffolds for adult mouse neural stem cell 3-dimensional cultures. PLoS One. 2006; 1:e119.
17. Allen P, Melero-Martin J, Bischoff J. Type I collagen, fibrin and PuraMatrix matrices provide permissive environments for human endothelial and mesenchymal progenitor cells to form neovascular networks. J Tissue Eng Regen Med. 2011; 5:e74–e86.
18. Thonhoff JR, Lou DI, Jordan PM, et al. Compatibility of human fetal neural stem cells with hydrogel biomaterials in vitro. Brain Res. 2008;1187:42–51.
19. Lee JH, Yu HS, Lee GS, Ji A, et al. Collagen gel three-dimensional matrices combined with adhesive proteins stimulate neuronal differentiation of mesenchymal stem cells. J R Soc Interface. 2011;8:998–1010.
20. Hauser CA, Zhang S. Designer self-assembling peptide nanofiber biological materials. Chem Soc Rev. 2010;39:2780–2790.
21. Kam L, Shain W, Turner JN, Bizios R. Selective adhesion of astrocytes to surfaces modified with immobilized peptides. Biomaterials. 2002;23:511–515.
22. Li Q, Chau Y. Neural differentiation directed by self-assembling peptide scaffolds presenting laminin-derived epitopes. J Biomed Mater Res A. 2010;94:688–699.
23. Cunha C, Panseri S, Villa O, et al. 3D culture of adult mouse neural stem cells within functionalized self-assembling peptide scaffolds. Int J Nanomed. 2011;6:943–955.
24. Ortinau S, Schmich J, Block S, et al. Effect of 3D-scaffold formation on differentiation and survival in human neural progenitor cells. Biomed Eng Online. 2010;9:70.
25. Liedmann A, Rolfs A, Frech MJ. Cultivation of human neural progenitor cells in a 3-dimensional self-assembling peptide hydrogel. J Vis Exp. 2012;e3830.
26. Donato R, Miljan EA, Hines SJ, et al. Differential development of neuronal physiological responsiveness in two human neural stem cell lines. BMC Neurosci. 2007;8:36.
27. Morgan PJ, Ortinau S, Frahm J, et al. Protection of neurons derived from human neural progenitor cells by veratridine. Neuroreport. 2009;20:1225–1229.
28. Morgan PJ, Liedmann A, Hübner R, et al. Human neural progenitor cells show functional neuronal differentiation and regional preference after engraftment onto hippocampal slice cultures. Stem Cells Dev. 2011 Dec 23 [Epub ahead of print]; doi:10.1089/scd.2011.0335.
29. Hoffrogge R, Mikkat S, Scharf C, et al. 2-DE proteome analysis of a proliferating and differentiating human neuronal stem cell line (ReNcell VM). Proteomics. 2006;6:1833–1847.
30. Hübner R, Schmöle AC, Liedmann A, et al. Differentiation of human neural progenitor cells regulated by Wnt-3a. Biochem Biophys Res Commun. 2010;400:358–362.
31. Mazemondet O, Hübner R, Frahm J, et al. Quantitative and kinetic profile of Wnt/beta-catenin signaling components during human neural progenitor cell differentiation. Cell Mol Biol Lett. 2011;16:515–538.
32. Schmöle AC, Brennführer A, Karapetyan G, et al. Novel indolylmaleimide acts as GSK-3beta inhibitor in human neural progenitor cells. Bioorg Med Chem. 2010;18:6785–6795.
33. PuraMatrix™ Peptide Hydrogel Guidelines for Users. Available at www.bdbiosciences.com/external_files/dl/doc/manuals/live/web_enabled/354250Lpug.pdf
34. Markwardt SJ, Wadiche JI, Overstreet-Wadiche LS. Input-specific GABAergic signaling to newborn neurons in adult dentate gyrus. J Neurosci. 2009;29:15063–15072.
35. Hirst AR, Escuder B, Miravet JF, Smith DK. High-tech applications of self-assembling supramolecular nanostructured gel-phase materials: From regenerative medicine to electronic devices. Angew Chem Int Ed Engl. 2008;47:8002–8018.
36. Richardson RM, Fillmore HL, Holloway KL, Broaddus WC. Progress in cerebral transplantation of expanded neuronal stem cells. J Neurosurg. 2004;100:659–671.
37. Kim SU, de Vellis J. Stem cell-based cell therapy in neurological diseases: A review. J Neurosci Res. 2009;87:2183–2200.
38. Kleinman HK, Martin GR. Matrigel: Basement membrane matrix with biological activity. Semin Cancer Biol. 2005;15: 378–386.
39. Choi JS, Yang HJ, Kim BS, et al. Human extracellular matrix (ECM) powders for injectable cell delivery and adipose tissue engineering. J Control Release. 2009;139:2–7.
40. Achyuta AK, Cieri R, Unger K, Murthy SK. Synergistic effect of immobilized laminin and nerve growth factor on PC12 neurite outgrowth. Biotechnol Prog. 2009;25:227–234.

41. Lim SH, Liu XY, Song H, et al. The effect of nanofiber-guided cell alignment on the preferential differentiation of neural stem cells. Biomaterials. 2010;31:9031–9039.
42. Martinez-Ramos C, Lainez S, Sancho F, et al. Differentiation of postnatal neural stem cells into glia and functional neurons on laminin-coated polymeric substrates. Tissue Eng Part A. 2008;14:1365–1375.
43. Yao L, Damodaran G, Nikolskaya N, et al. The effect of laminin peptide gradient in enzymatically cross-linked collagen scaffolds on neurite growth. J Biomed Mater Res A. 2010;92: 484–492.
44. Engler AJ, Sen S, Sweeney HL, Discher DE. Matrix elasticity directs stem cell lineage specification. Cell. 2006;126:677–689.
45. Saha K, Keung AJ, Irwin EF, et al. Substrate modulus directs neural stem cell behavior. Biophys J. 2008;95:4426–4438.
46. Leipzig ND, Shoichet MS. The effect of substrate stiffness on adult neural stem cell behavior. Biomaterials. 2009;30:6867–6878.
47. Zhang S. (2008). Designer self-assembling Peptide nanofiber scaffolds for study of 3-D cell biology and beyond. Adv Cancer Res 99:335–362.
48. Bordey A. Enigmatic GABAergic networks in adult neurogenic zones. Brain Res Rev. 2007;53:124–134.
49. Bordey A. Adult neurogenesis: Basic concepts of signaling. Cell Cycle. 2006;5:722–728.
50. Ge S, Pradhan DA, Ming GL, Song H. GABA sets the tempo for activity-dependent adult neurogenesis. Trends Neurosci. 2007;30:1–8.
51. Platel JC, Bordey A. [Function of NMDA receptors activated by astrocytic glutamate on postnatal neurogenesis]. Med Sci (Paris). 2010;26:675–677. (In French.)
52. Wegner F, Kraft R, Busse K, et al. Glutamate receptor properties of human mesencephalic neural progenitor cells: NMDA enhances dopaminergic neurogenesis in vitro. J Neurochem. 2009;111:204–216.
53. Suzuki M, Nelson AD, Eickstaedt JB, et al. Glutamate enhances proliferation and neurogenesis in human neural progenitor cell cultures derived from the fetal cortex. Eur J Neurosci. 2006;24:645–653.
54. Kaneko K. Characterization of stem cells and cancer cells on the basis of gene expression profile stability, plasticity, and robustness: Dynamical systems theory of gene expressions under cell-cell interaction explains mutational robustness of differentiated cells and suggests how cancer cells emerge. Bioessays. 2011;33:403–413.
55. Baghbaderani BA, Behie LA, Mukhida K, et al. New bioengineering insights into human neural precursor cell expansion in culture. Biotechnol Prog. 2011;27:776–787.
56. Kiss JZ, Rougon G. Cell biology of polysialic acid. Curr Opin Neurobiol. 1997;7:640–646.
57. Seki T, Arai Y. Distribution and possible roles of the highly polysialylated neural cell adhesion molecule (NCAM-H) in the developing and adult central nervous system. Neurosci Res. 1993;17:265–290.
58. Olsen RW, Sieghart W. GABA A receptors: Subtypes provide diversity of function and pharmacology. Neuropharmacology. 2009;56:141–148.
59. Mayer-Proschel M, Kalyani AJ, Mujtaba T, Rao MS. Isolation of lineage-restricted neuronal precursors from multipotent neuroepithelial stem cells. Neuron. 1997;19:773–785.
60. Mujtaba T, Piper DR, Kalyani A, et al. Lineage-restricted neural precursors can be isolated from both the mouse neural tube and cultured ES cells. Dev Biol. 1999;214:113–127.
61. Carpenter MK, Inokuma MS, Denham J, et al. Enrichment of neurons and neural precursors from human embryonic stem cells. Exp Neurol. 2001;172:383–397.
62. Jungling K, Nagler K, Pfrieger FW, Gottmann K. Purification of embryonic stem cell-derived neurons by immunoisolation. FASEB J. 2003;17:2100–2102.
63. Wernig M, Tucker KL, Gornik V, et al. Tau EGFP embryonic stem cells: An efficient tool for neuronal lineage selection and transplantation. J Neurosci Res. 2002;69:918–924.
64. Schmandt T, Meents E, Gossrau G, et al. High-purity lineage selection of embryonic stem cell-derived neurons. Stem Cells Dev. 2005;14:55–64.

Address correspondence to:
Moritz Frech, PhD
Albrecht-Kossel-Institute for Neuroregeneration
University of Rostock
Gehlsheimer Strasse 20
18147 Rostock
Germany

E-mail: moritz.frech@med.uni-rostock.de